Linear basis for metallic and iridescent colors

José M. Medina

Center for Physics, University of Minho, Campus de Gualtar, 4710-057 Braga, Portugal (jmanuel@fisica.uminho.pt)

Received 8 July 2008; accepted 17 September 2008;
posted 19 September 2008 (Doc. ID 98354); published 15 October 2008

I have examined the correlation structure in goniochromism by principal-component analysis. Reflectance spectra were collected in synthetic samples that reproduce metallic, nacreous, and iridescent effects under different viewing angles. Although three principal components take into account 99% of the variance, between seven and eight are needed to reach 99.99%. The results were also confirmed by analyzing each viewing condition separately. It was found that although the viewing angle does not modify the first three basis functions, it affects the higher-order ones. These angle-dependent effects can be attributed to optical interference flakes. The implications for pigment identification are discussed. © 2008 Optical Society of America

OCIS codes: 330.1730, 310.1620, 310.3915, 310.6188, 260.3160, 120.5700.

1. Introduction

Modern man-made coatings have included special pigments and dyes for different technological and commercial issues. Cosmetics, automotive coatings, and security inks commonly contain goniochromism effects (also called goniochromatism) [1,2], in the same way as opals, bird feathers, or butterfly wings [3–5]. That is, they present remarkable color changes under different illumination-viewing conditions [6–13]. The origin of these striking effects comes from specific photonic structures assembled at the micrometer or submicrometer scales [7]. Their optical behavior differs from conventional absorbing pigments in two basic respects. First, they manipulate the flow of light by thin-film interference, diffraction, or scattering. Second, color is formulated in accordance with the laws of additive mixing [7,9,12,14]. Both electron and optical microscopy provide valuable information about their form, size, or opacity, whereas their spectra are mainly captured by the bidirectional reflectance distribution function (BRDF). Regarding the latter, few standards of gonioappearance have been developed. Basically the calculation of the BRDF is simplified by fixing certain angles of illumination and detection measurement. Each pair of illumination-detection angles specifies different geometries of measurement [6,7,11,15–17]. As a consequence, spectral reflectance analysis is made under each geometric condition separately. This provides a large quantity of data and complicates color analysis. However, reflectance functions are very similar in shape and present smooth changes over a broadband range of measurement geometries [6,7,9,10,12].

The aim of the present work was to examine the interrelations between spectra in goniochromism by spectral data reduction analysis. As a first step, I sought to examine object reflectance from those materials that imitate metal-like, nacreous, or pearlescent as well as iridescent effects (hue shifts). Their spectra are representative of goniochromism [7]. In color science, traditional approaches have decomposed illuminants and object reflectance into low-dimensional vector spaces. That is, they can be expanded in a finite series, usually a linear combination of a small number of independent basis functions [10,18–22]. In matte and glossy color surfaces, five to eight basis functions are needed for optimal reproduction of artificial and natural reflectance, a property derived computationally [10,18,20–22] and by psychophysical experiments [23]. In this study, the reflectance spectra of a collection containing synthetic (automotive) goniochromatic painted samples were analyzed by principal-component analysis (PCA). PCA is one common way to decorrelate reflectance into few independent

0003-6935/08/305644-10$15.00/0

(uncorrelated) components that maximize the variance accounted for. This technique has been widely used for dimensionality reduction [21,24] and in the study of color databases [20,22,24–26]. In color technology, the dimension and the complete set of basis functions are important to identify and reduce the number of colorants [24]. Although previous works on PCA have analyzed the optical behavior and measuring geometries [10,17], they have not examined the adequacy of linear models using the standards of gonioappearance. Here I attempt to determine if a few suitable colorants have the ability to cover the entire reflectance spectrum derived from goniochromism. If reflection from metallic and iridescent surfaces is as redundant as from uniform color surfaces, linear approaches may produce similar results. I also discuss PCA for pigment identification. In colorant estimation, one normally seeks a transformation derived from an optical model (e.g., in subtractive color mixing, the Kubelka–Munk theory), where linear algebra and vector analysis recover the spectral information of the physical colorants [24,27]. However, in goniochromatic coatings, both interference and conventional absorbing pigments are often present [7,9]. PCA provides the spectral characterization of colorants when they are added together and offers the possibility of using vector addition in the reflectance space [24,25]. This simulates additive color mixing from interference pigments. Hence I examine the linear reconstruction of the original spectral reflectance spectra when these interference pigments are present alone or with standard absorbing colorants. In paint formulation, this analysis is useful to identify special color mixtures [9].

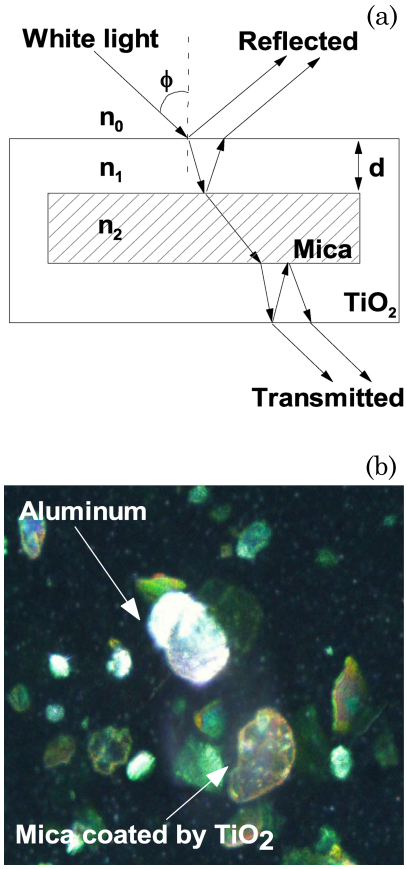

Fig. 1. (Color online) (a) Schematic of an interference flake (mica coated by TiO_2). Fringes of equal inclination are generated at the specular reflection by the metal oxide layer. Those rays not reflected are transmitted to the next interface. (b) Microscopic image of a typical metallic-green coating containing lenticular aluminum and pearl red-green interference pigments (50×, dark-field illumination).

2. Theoretical Background

A. Color from Synthetic Multilayer Reflectors

Current coating technology produces thin films that contain different types of pigments. One means of classification deals with their reflective properties. At least three categories of pigment can be considered. The first is conventional absorbing pigment, which provides color and scatters most light diffusely in all directions. The second is illustrated by metal flakes, which act like mirrors (e.g., aluminum) and are mainly responsible for changes in lightness. Finally, interference pigment, which scatters the flow of light by interference, produces selective color reflection [7]. Regarding the latter, a typical example is represented in Fig. 1(a). Flakes of mica (refractive index n_2) are coated with metal oxide. Titanium dioxide (TiO_2) is normally used with thickness d and refractive index n_1. These flakes, or platelets, are immersed in a vehicle or binder with refractive index n_0, producing a three-layer reflector of alternate high and low refractive indices (i.e., $n_0 < n_2 < n_1$).

Incident white light of illumination angle ϕ from the normal is reflected and transmitted across layers. Constructive and destructive interference in the reflected light is wavelength specific. Maxima and minima are produced by evaluating the phase change due to the optical path length difference of two consecutive rays. There is also an additional 180° phase shift when reflection occurs from a low-to-high refractive index media (i.e., in this specific case, from the binder to the TiO_2 layer) [7,9,12,13,28]:

$$(\text{Maxima})\lambda = \frac{2d[n_1^2 - n_0^2\sin^2(\phi)]^{1/2}}{\left(m + \frac{1}{2}\right)}, m = 0, \pm 1, \pm 2, \ldots, \quad (1)$$

$$(\text{Minima})\lambda = \frac{2d[n_1^2 - n_0^2\sin^2(\phi)]^{1/2}}{m}, m = \pm 1, \pm 2, \ldots, \quad (2)$$

where λ is the wavelength of the reflected light in the vacuum, and m is an index that accounts the order of

interference. The reflected rays are parallel and can be focused at a specific position by any convergent optical system such as the human eye. Hence the perceived color often depends on the viewing angle [7,9,10,12,17]. At the same time, Eq. (1) indicates that the relative angle between the illumination source and the surface, together with the optical thickness of the film ($n_1 d$), can also control the spectral properties of the perceived color [7,9,12]. There is no phase change between two consecutive transmitted rays from a high-to-low refractive index media (i.e., from TiO_2 to the binder). This implies that transmitted maxima correspond to minima in the reflected light and vice versa [7,9,28]. For example, if the wavelength of reflected light is reddish, the transmitted light will correspond to the complementary color within the wavelength range of green. Transmitted light goes to the next parallel interference layer, producing reflected rays of equal inclination by deeper flakes (multilayer reflectors). These rays contribute to increased reflection in the specular direction, producing a pearlescent luster [7,28]. Some diffuse reflectance is due to edges and surface imperfections, but the major contribution comes from background (white or black) and, if present, classical absorbing pigments. As in natural coatings, the combination with conventional pigments enhances the variation in color with the angles of illumination and observation. If the colorants are similar, the mixture of interference and absorbing pigments with overlapping spectral bands enhances the reflectance factor (e.g., pearl-green with green), whereas color-opponent mixtures (e.g., pearl-red with green) show the opposite effect [9]. Figure 1(b) presents a microscopic image of a typical metallic-green coating. Pearl mica and aluminum flakes are, on average, oriented parallel to the surface [7,10,29]. In this particular case, their characteristic lengths are very similar and range between 11 and 36 μm. Interference platelets clearly show a color range from bluish through greenish to reddish (pearl red-green), but full spectral information is represented by the BRDF at different illumination-viewing geometries [7–9,12].

3. Methods

A. Measurement Geometries of Metallic Coatings

The measurement and analysis of the BRDF in goniochromatic surfaces are usually made by multiangle spectrophotometers [7,8]. Modern colorimetry has provided methods to capture goniochromism. Assuming homogeneous samples, Fig. 2 indicates a schematic representation of a prototype five-angle spectrophotometer. In general, at a fixed illumination angle measured from the normal, a possible viewing coordinate system is defined from the specular (glossy) reflection.

Three to five viewing geometries (aspecular angles, γ) are suitable to describe metallic paints [15–17,30]. These angles are classified as near-specular, face, or normal incidence and far from specular, or "flop," angles. The Deutsches Institut für Normung (DIN) recommends the use of three aspecular angles of 25°, 45°, 75°, and optionally 110°, whereas the American Society for Testing Materials prescribes three aspecular angles of 15°, 45°, and 110° [15,16]. In both standards, the illumination angle is fixed at 45° from the normal (see Fig. 2). In nearly matte surfaces, the BRDF is simplified to one measuring illumination-viewing geometry (e.g., Commission Internationale de l'Éclairage, International Commission on Illumination [CIE] 45°/0°). Note that this is similar to choosing the viewing aspecular angle of $\gamma = 45°$ in the original goniochromatic configuration [8,14].

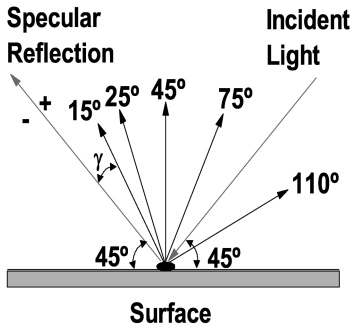

Fig. 2. Schematic of a five-angle spectrophotometer. Illumination source is fixed at the standard geometry of 45° from the normal. Measuring geometries are defined from specular reflection (aspecular viewing angles) at 15°, 25°, 45°, 75°, and 110°.

B. Samples and Instrumentation

The reflectance database consisted of 108 different goniochromatic samples provided by C. Vignolo (BASF). This collection corresponds to different reference panels used in color reproduction from automotive coating suppliers in Europe. Paints were uniformly spread on panels. They consisted of a basecoat containing the pigments in a binder and a transparent topcoat lacquer. The topcoat protects and provides a glossy aspect. For each sample, the relative pigment concentration was enough to hide the substrate completely. Panels contained an unknown pigment gamut that included the combination of metallic, interference, and conventional diffuse pigmentation. The experimental device consisted of an X-Rite MA68-II portable multiangle spectrophotometer. This device is specialized for measurement on goniochromatic paints and compatible with the standards of gonioappearance. That is, the illumination source was 45° from normal, and aspecular viewing angles were at 15°, 25°, 45°, 75°, and 110° (see Fig. 2). Instrument calibration was done to perform white and zero reflection measurement using a white ceramic tile and a black trap, respectively. Both were provided by the manufacturer, and a calibration procedure was done periodically in accordance with the operator's manual. For each goniochromatic sample, reflectance at each aspecular angle was averaged from a minimum of five consecutive readings. The

area was rectangular with dimensions 105 mm× 150 mm. In some samples containing a high concentration of metal flakes, the measured reflectance factor (defined from the white reflection tile) was far greater than unity at $\gamma = 15°$ or in some cases at $\gamma = 25°$ (8.6% of all measurements exceed unity). This is possible because metal and interference flakes reflect most of the light at the specular direction [see Eqs. (1) and (2) and Fig. 1(a)]. In all the samples, reflectance spectra were within the range of 0–400% (defined from the incident flux beam). This provides a total of 540 reflectance measures.

C. Principal-Component Analysis and Colorimetric Evaluation

Each spectral reflectance at each specular angle was measured within the visible range from 400 to 700 nm in 10 nm steps. In this case, each spectral reflectance factor was examined as a 31-dimensional vector. PCA excludes those dimensions (wavelengths) with negligible variance of the data set. The correlation matrix is calculated in the eigenvector or basis coordinate system. If the mean reflectance vector, $\bar{\mathbf{R}}$, is within the range spanned by the first few eigenvectors, the linear model generates each vector reflectance sample $\mathbf{R_j}$ from a finite number of the eigenvectors $\mathbf{S_i}$ according to the following matrix expression [24,26]:

$$\mathbf{R_j} \cong \sum_{i=1}^{m} \alpha_i \mathbf{S_i}, j = 1, \ldots, 540; m \le 31, \tag{3}$$

where α_j are the coordinates in the eigenvector basis and denote the principal components. Each principal component has an associated eigenvalue. Eigenvalues provide the variance measured, and they are usually taken as a criterion to select the corresponding basis element [24]. The reconstruction of the spectral reflectance database was examined by Eq. (3). The goodness-of-fit between the original (R) and the reconstructed reflectance (R') was evaluated by the root mean square (RMS) error $\{\sum_{i=1}^{31}[R(\lambda_i) - R'(\lambda_i)]^2\}^{1/2}$ [22,24]. Color differences were evaluated using the CIE 10° standard observer under the illuminant D65 [14]. The DIN 6175-2 color difference formula (ΔE DIN) was used [15]. This formula is specialized for the color evaluation of metallic coatings at different aspecular viewing angles. For chromatic coatings, ΔE DIN can be expressed as follows:

$$\Delta E(\gamma) = \left\{ \left[\frac{\Delta \mathrm{L}}{g_{\mathrm{L}} S_{\mathrm{L}}(\gamma)} \right]^2 + \left[\frac{\Delta \mathrm{C}}{g_{\mathrm{C}} S_{\mathrm{C}}(\gamma)} \right]^2 + \left[\frac{\Delta \mathrm{H}}{g_{\mathrm{H}} S_{\mathrm{H}}(\gamma)} \right]^2 \right\}^{1/2}, \tag{4}$$

where S_{L}, S_{C}, and S_{H} and g_{L}, g_{C}, and g_{H} indicate different weights associated with lightness $\Delta \mathrm{L}*$, chroma $\Delta \mathrm{C}*$, and hue differences $\Delta \mathrm{H}*$, respectively [15]. S values depend on the aspecular angle, and g values are specific for different paint applications. There is a similar expression for nearly achromatic coatings using $\Delta \mathrm{L}*$, $\Delta \mathrm{a}*$, and $\Delta \mathrm{b}*$ and their corresponding weights [15]. The transition area between achromatic and chromatic coatings is evaluated by a weighted sum of both color differences formulas. In both chromatic and achromatic zones, ΔE values higher than unity are considered above one just noticeable difference [15].

4. Results

A. Spectral Reflectance Factor of Goniochromatic Coatings

Figure 3 (left column) indicates in a semilogarithmic plot, the spectral reflectance factor of four representative coatings at different aspecular angles ($\gamma = 15°$, 25°, 45°, 75°, and 110°). Samples in Figs. 3(a) and 3(b) correspond to metallic coatings and contain a high concentration of aluminum flakes (mirrorlike reflectors). Samples in Figs. 3(c) and 3(d) represent the opposite. That is, they contain more interference than aluminum pigments. Metal flakes produce nearly flat spectra and mainly scale the reflectance factor in the vertical axis. It decreases from near-specular to flop angles. In comparison, the spectral properties in samples containing a high concentration of interference platelets were different. The reflectance factor has different minima in accordance with the spectral properties of the pigments. It also decreases but moves horizontally far from specular reflection. In all examples, the spectral reflectance factors are very similar at different viewing angles but not identical. Using a normalization procedure (e.g., the norm of square-integrable functions) [21], they resemble each other, but they do not superpose at different viewing angles. The wavelength at which reflectance factor are maxima (λ_{MAX}) showed poor or null dependence upon the viewing angle in those samples with a high concentration of metal flakes [Figs. 3(a) and 3(b), central column]. On the contrary, there was a hue modulation in those samples with a major contribution of mica-TiO_2 platelets [Figs. 3(c) and 3(d), central column]. Color coordinates also illustrate goniochromism (Fig. 3, right column). The CIE 1976 L * a * b* (CIELAB) color space was used. CIELAB values were calculated using the CIE 10° standard observer and taking as reference the illuminant D65 [14]. Metal-based samples produce significant lightness (L*) changes at different viewing angles [Figs. 3(a) and 3(b), left column]. These changes are less pronounced in interference-based coatings, where major variations correspond to a * b* values [Figs. 3(c) and 3(d), left column].

Figure 4 presents the color gamut in the CIELAB color space embraced by all the goniochromatic painted panels at all the viewing angles. Color data comprise a range of 31.5 CIELAB units in lightness, whereas the range expanded in chromaticity was 17.8, 11.5, 15, and 16.4 CIELAB units for red ($a* > 0$), green ($a* < 0$), yellow ($b* > 0$), and blue ($b* < 0$), respectively.

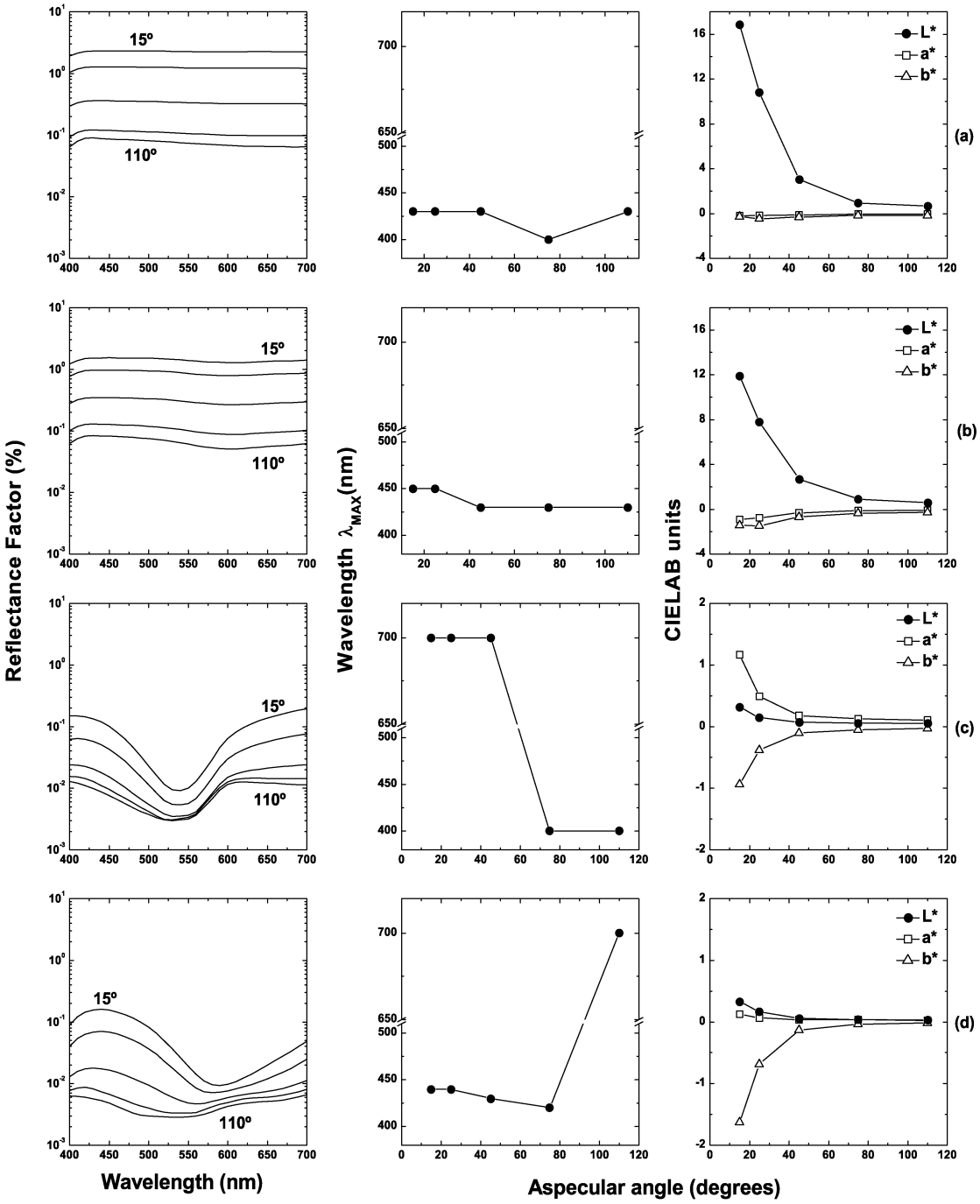

Fig. 3. Spectral properties and colorimetric values of four representative goniochromatic samples. (a) and (b) Examples containing high concentration of metal flakes (metallic coatings). (c) and (d) Examples containing optical interference flakes (pearlescent coatings). Left column: Semilogarithmic plot of the spectral reflectance curves. Reflectance factors are indicated for each aspecular viewing geometry separately at 15°, 25°, 45°, 75°, and 110°. Central column: Wavelength at maximum reflectance in relation to the viewing aspecular angle. Right column: CIELAB values for different aspecular angles. Data were calculated using CIE 10° standard observer and D65 illuminant.

B. Global Basis

PCA was done in goniochromatic materials using the 540 spectral reflectance factors measured under all the viewing geometries (aspecular angles of $\gamma = 15°$, 25°, 45°, 75°, and 110°). Table 1 provides the cumulative percentage of variance accounted with the first eight principal components. Although three principal components take into account more than 99% of the total variance, it was necessary to include four or five components more to reach 99.99%. PCA was also done on a simulation that imitates color uniform surfaces. To generate these spectra, it was assumed that the perceived color was nearly independent on the illumination-viewing

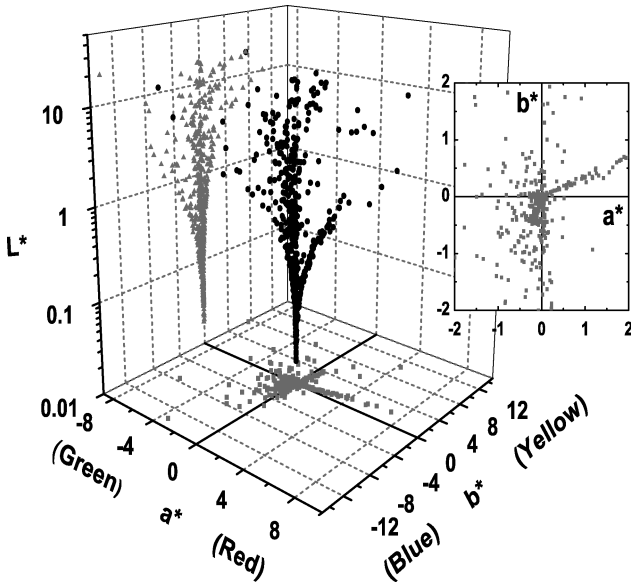

Fig. 4. CIELAB values of the synthetic goniochromatic surfaces for all the viewing angles measured. Solid black symbols represent the color coordinates in the three-dimensional color space. Solid gray symbols represent the projections in the a∗b∗ and L∗b∗ planes. Data were calculated using CIE 10° standard observer and D65 illuminant. Lightness values are in logarithmic units. The inset shows an amplification of the chromaticity coordinates in the a∗b∗ plane.

angles so that the standard CIE 45°/0° measuring geometry is sufficient to characterize them [8,14]. That is similar to choosing spectral reflectance spectra only at the aspecular angle $\gamma = 45°$ from the original database.

Although the percent of variance explained by the first two principal components increases in the simulated color uniform data (goniochromatic, 88.12%, 7.56%; uniform, 88.81%, 8.29%), it decreases in the third principal component (goniochromatic, 3.99%; uniform, 2.34%, respectively). It is concluded that a minimum of seven or eight principal components are also necessary to explain around 99.99% of total variance at $\gamma = 45°$ (see Table 1). Comparing their associated eigenvectors in both conditions (i.e., goniochromatic versus uniform), the first three eigenvectors differ slightly from those obtained under goniochromatism. However, there was a wavelength shift in the subsequent basis functions for goniochromatic materials, suggesting a possible dependency upon the viewing angle.

C. Effect of the Viewing Angle

PCA on reflectance spectra was also done with the 108 spectral reflectance factors obtained at each aspecular angle separately. Figure 5 presents the eigenvectors associated with the first eight principal components (around 99.99% of total variance). Their spectra are modulated around the mean so that reflectance curves represent statistical values or weights. To simplify the view, eigenvectors were only represented at near-specular, $\gamma = 15°$ (solid curves); face, $\gamma = 45°$ (dashed curves); and far from specular, or flop, angles $\gamma = 110°$ (dash-dotted curves). Table 2 indicates the cumulative percent of variance explained by the first eight principal components at $\gamma = 15°$, 25°, 45°, 75°, and 110° aspecular angles separately. The first three principal components accounted more than 99% of the total variance. Their spectra characteristics were only slightly affected by the viewing geometry. The associated eigenvector of the first principal component reflects light at all wavelengths by almost the same amount and can be associated with metal flakes [see also Figs. 3(a) and 3(b)] [10]. This implies that around 85–90% of variance could be attributable to lightness changes (see Table 2). The two subsequent eigenvectors are peaked at different wavelengths and represent the contribution of different conventional pigmentation within the basecoat.

In the next five basis functions, there was a wavelength shift of the maxima within 20–80 nm between near-specular ($\gamma = 15°$) to face ($\gamma = 45°$) or flop angles ($\gamma = 110°$). This hue shift also compresses the eigenvectors to narrower bands at different wavelength intervals far from the specular direction (see Fig. 5, basis functions labeled from 4 to 8). The analysis of the cross-correlation function helps identify relations when moving from near to far from the specular reflection as a function of wavelength intervals (i.e., lag $\Delta\lambda$ nm). Hence, for each basis function, the cross-correlation function was calculated between $\gamma = 15°$ and $\gamma = 110°$ using the discrete Fourier transform [31]. Positive and negative lag values indicate that both functions were compared when the first one was shifted to the right of the second and vice versa, respectively [31]. Basis functions 1, 2, and 3 have a correlation close to unity when they are superposed (i.e., 0.99, 0.98, and 0.94 at lag $\Delta\lambda = 0$, respectively). However, basis functions labeled from 4 to 8 lag in $\Delta\lambda$. Maximum correlation was found at lags $\Delta\lambda =$ 1(0.83), −3(−0.47), 4(0.83), 2(−0.66), and −2(−0.67), respectively. Given that colors from interference are fully developed close to the specular reflection, these spectra modifications are mainly expected for optical interference flakes [see also examples in Figs. 3(c) and 3(d) and Eqs. (1) and (2)] [7,9,10,12,17,28].

Table 1. Cumulative Percentage of Variance Accounted for the First Eight Principal Components (PCs) in Goniochromatic Materials Taking into Account All the Aspecular Viewing Angles Together: $\gamma = 15°$, 25°, 45°, 75°, and 110°[a]

	First PC	Second PC	Third PC	Fourth PC	Fifth PC	Sixth PC	Seventh PC	Eighth PC
Goniochromatic	88.12%	95.69%	99.69%	99.88%	99.95%	99.98%	99.99%	99.99%
Uniform	88.81%	97.11%	99.45%	99.84%	99.93%	99.96%	99.98%	99.99%

[a]Percentages are compared with PCA from a simulated database of uniform color patches (i.e., only $\gamma = 45°$).

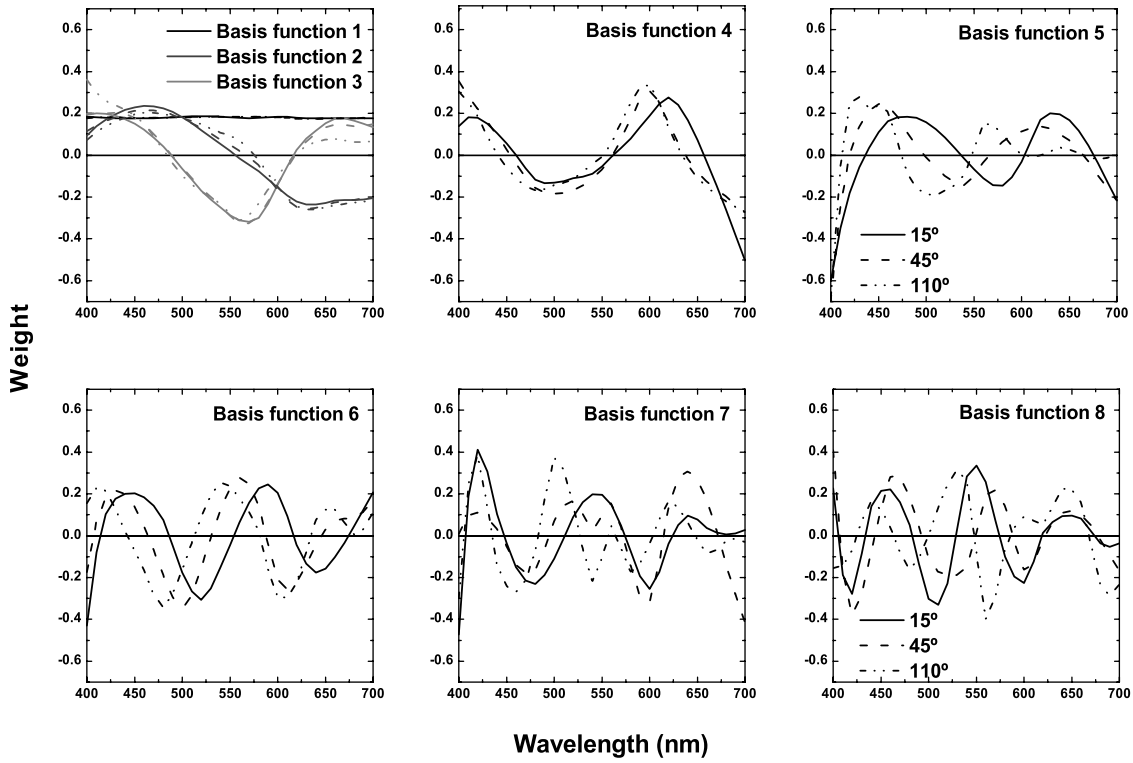

Fig. 5. PCA of goniochromatic samples at each viewing angle separately. Panels shows the first eight basis functions for near-specular (15°, solid curves), normal to the sample (45°, dashed curves), and close to the surface or far from specular (110°, dash-dotted curves). Top left corner: the first three basis functions were represented in the same panel. The first, second, and third bases are indicated by black, gray, and light gray, respectively.

D. Reconstruction of the Reflectance Spectra

At each aspecular angle, the mean reflectance factor was well fitted as a linear combination of the first eight basis functions. In all angles, the RMS error was less than 0.0007, and the percentage explained by the residuals was less than 1.1%. Therefore, Eq. (3) was used to fit the entire reflectance spectra [24,26]. Table 3 indicates the mean and maximum of the RMS error and the ΔE DIN estimated by the linear combination of the first three and first eight basis functions, respectively, at $\gamma = 15°$, 25°, 45°, 75°, and 110°, separately.

The linear combination of the first three basis functions is not accurate enough to represent reflectance curves. In some cases (14.25%), negative values were obtained at some wavelengths, and the reconstructed reflectance was rounded to zero at these intervals. The mean and maximum RMS error increased at $\gamma = 15°$ and 25°. This is also verified by the ΔE DIN color difference formula. Although mean values are less than unity, there are higher differences ($\Delta E > 1$), in many cases, at all aspecular angles. The reconstruction using the first eight eigenvectors includes those basis functions associated with interference platelets and was very good. In all cases, the RMS error was minimized, and the ΔE DIN color difference formula was less than 0.5. Exceptionally, there were five cases where reflectance had negative values at some wavelengths. This corresponds to reflectance curves very close to zero. The basis function 9 was added, and only one reflectance curve was composed by the linear combination of the first 10 basis functions. Figure 6(a) represents the reconstruction of two typical examples at $\gamma = 15°$ and $\gamma = 110°$. The left panel indicates a metallic-green sample, whereas the right panel corresponds to a metallic-red sample. Solid, dashed, and dash-dotted curves correspond to the original reflectance and the

Table 2. Cumulative Percentage of Variance Accounted for the First Eight Principal Components (PCs) in Goniochromatic Materials Taking into Account Each Viewing Angle Separately

	First PC	Second PC	Third PC	Fourth PC	Fifth PC	Sixth PC	Seventh PC	Eighth PC
$\gamma = 15°$	85.71%	94.61%	99.68%	99.88%	99.96%	99.98%	99.99%	99.99%
$\gamma = 25°$	87.49%	95.95%	99.64%	99.87%	99.95%	99.97%	99.98%	99.99%
$\gamma = 45°$	88.81%	97.11%	99.45%	99.84%	99.93%	99.96%	99.98%	99.99%
$\gamma = 75°$	90.50%	97.64%	99.06%	99.81%	99.90%	99.96%	99.98%	99.99%
$\gamma = 110°$	90.83%	97.41%	98.77%	99.74%	99.86%	99.94%	99.97%	99.99%

Table 3. Mean, Standard Error of the Mean (±1 SEM), and Maximum Root Mean Square Error and ΔE DIN of the Reconstructed Reflectance Spectra[a]

	Basis	$\gamma = 15°$	$\gamma = 25°$	$\gamma = 45°$	$\gamma = 75°$	$\gamma = 110°$
Mean RMS Error (±1 SEM)	3	0.36 (0.05)	0.18 (0.02)	0.062 (0.008)	0.037 (0.006)	0.033 (0.006)
	8	0.042 (0.004)	0.018 (0.002)	0.0071 (0.0007)	0.006 (0.001)	0.0050 (0.0007)
Maximum RMS Error	3	4.52	2.0	0.52	0.36	0.39
	8	0.26	0.14	0.04	0.06	0.04
Mean ΔE DIN (±1 SEM)	3	0.78 (0.06)	0.47 (0.03)	0.20 (0.02)	0.12 (0.02)	0.11 (0.02)
	8	0.034 (0.003)	0.015 (0.001)	0.0039 (0.0004)	0.0028 (0.0005)	0.0023 (0.0004)
Maximum ΔE DIN	3	3.91	1.97	1.91	1.22	1.20
	8	0.34	0.13	0.02	0.04	0.03

[a]Values are estimated by the linear combination of the first three and the first eight basis functions at each viewing angle separately.

linear combination of the first three and first eight basis functions, respectively.

For the same examples, Fig. 6(b) represents the recovered reflectance curves by the linear combination of the eigenvectors 1, 4, 5, 6, 7, and 8 (dashed curves). This represents hypothetical panels containing only those metal and interference pigments from the original goniochromatic samples without contribution of any conventional absorbing pigment. As expected, the simulated reflectance from interference multilayers is more pronounced close to the specular reflection ($\gamma = 15°$). The reconstructed reflectance suggests the existence of reddish-greenish and yellowish-purplish mica in the metallic-green and

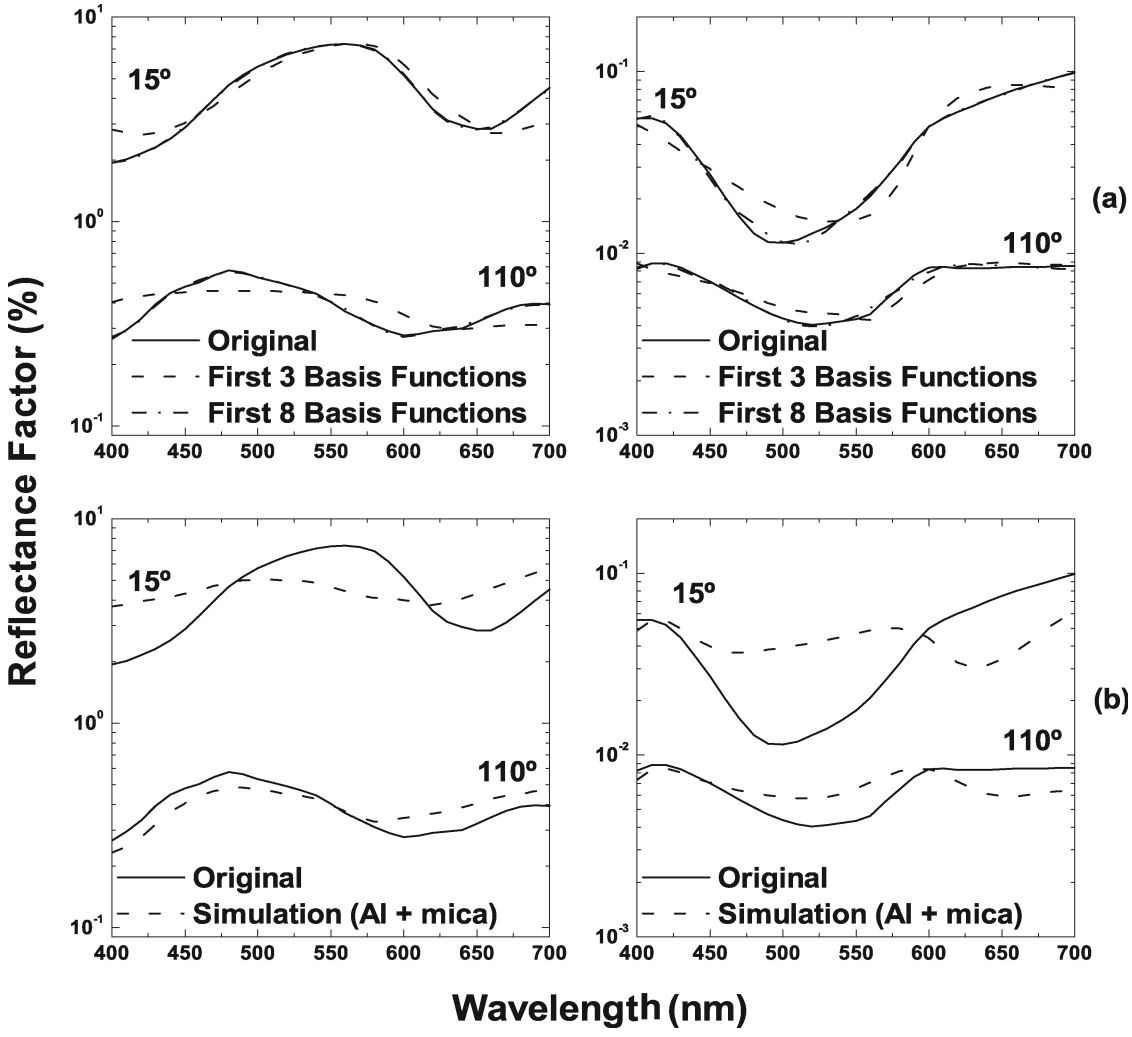

Fig. 6. Examples of a reconstruction of a metallic-green (left column) and a metallic-red (right column) goniochromatic samples at 15° and 110°, separately. Solid curves represent the original reflectance functions. Dashed and dash-dotted curves represent the reconstruction using the linear combination of the first three and first eight basis functions, respectively. (b) Examples of reconstruction (dashed curves) of the same examples using only those basis functions associated with aluminum (Al) and pearl-mica pigments. Solid curves represent the original reflectance functions.

metallic-red samples, respectively. The spectral information obtained from PCA reinforces the analysis by optical microscopy. In the metallic-green example, a microscopic image of the original painted panel is represented in Fig. 1(b). Figure 6(b) (left panel) suggests the existence of one type of pearl red-green pigment. The color mixing effects with conventional absorbing colorants are examined together with the original reflectance function (solid curves). In the metallic-green sample, the original spectral reflectance factor mainly enhances the perceived color in the greenish area and shows a displacement of the maximum to the yellowish part of the visible spectrum. This suggests the addition of green or yellow color pigments with overlapping spectral bands. In the metallic-red sample, there is a reduction in the original reflectance factor in the bluish-greenish area. The maximum also enhances, showing a displacement to the reddish part of the spectrum. This suggests a color mixture that contains red color pigments with remote spectral bands in relation to the pearl-mica pigments [9].

5. Discussion

Based on PCA, the results show that linear models of surface color perception are good approaches in modeling reflectance and goniochromism. The analysis on synthetic materials supports the conclusion that most of redundancies in goniochromism can be explained by a finite set of basis functions. Fixing the angle of illumination, the first three principal components account for more than 99% of total variance (see Tables 1 and 2). In accordance with the goniochromatic samples analyzed, the origin of their corresponding basis 1, 2, and 3 can be associated with lightness changes (i.e., metal flakes) [10] and the spectral characteristics of a few conventional absorbing pigments.

However, three principal components do not cover all the spectra analyzed. It was necessary to add four or five more, giving a minimum of seven or eight principal components to account for 99.99% of total variance. This result was also confirmed for each viewing angle separately (see Table 2). The five added basis functions are narrower and contain more peaks as compared with the first three. PCA at each aspecular angle reveals that they were fully developed close to the specular reflection. That is, they experienced narrower bandwidths and displaced maxima as the viewing angle moved close to the surface (see Fig. 5, basis functions labeled from 4 to 8). The wavelength shifts observed (between 20 and 80 nm) cause detectable changes above the wavelength discrimination threshold [14] and are related to iridescence from multilayer reflectors [see Eqs. (1) and (2)]. The number of basis functions needed for spectra reproduction depends on the accuracy of the specific application [24]. Based on the RMS error and the DIN 6175-2 color difference formula, the first eight and exceptionally the first nine or ten eigenvectors are adequate for the spectral reconstruction of the original goniochromatic database (see Table 3). Previous works have concluded that a similar number of dimensions are required in the analysis of uniform color samples [18,20–22] as well as in perceptual tasks [23].

Therefore a colorant database with a finite number of interference pigments (in this case, a minimum of seven) could recover any reflectance dataset derived from goniochromatism. This analysis excludes the consecution of special texture effects from metallic and pearl-mica pigments [1,32]. The spectral properties of these hypothetical pigments could be uncovered using a matrix transform of the estimated eigenvectors. However, in the current spectra space, the reflectance factor does not scale linearly (see Fig. 3), and a transformation is commonly desirable [24,27]. Although certain modeling approaches have examined the goniochromatic properties of some microstructures in biology [33,34], current reflection models are not accurate enough to describe color generated by metal flakes, photonic structures, and conventional absorbing pigments simultaneously [8,29,35]. PCA in goniochromism offers the possibility of testing whether our current colorant database can identify the spectral properties of pigments from their mixtures in any color sample. This is important in industrial color reproduction [7,8]. Close to the specular reflection (e.g., $\gamma = 15°$), the reconstruction of the spectral reflectance factor using only those basis functions associated with metal and interference flakes complements the evaluation with optical microscopy [see Figs. 1(b) and 6(b)]. Comparison between the simulated and original reflectance functions permits examination of color mixing effects with standard colorants [see Fig. 6(b)] [9]. In accordance with Eqs. (1) and (2), the illumination angle can also control the spectral characteristics of reflected light by interference [28]. Previous works have reported similar dependent wavelength effects in both reflectance spectra and colorimetric values [9,12]. Therefore the potential influence of the illuminant position on the vector bases inferred from interference merits further investigation. New gonioappearance standards are also required [9,12].

I thank C. Vignolo (BASF Coatings AG) for providing reflectance measurements. I am also grateful to S. Nascimento (University of Minho), J. A. Diaz (University of Granada), and K. Norwich (University of Toronto) for helpful discussions and comments. This work was supported by the Fundação para a Ciência e Tecnologia and by the Center for Physics, University of Minho, Portugal.

References

1. C. S. McCamy, "Observation and measurement of the appearance of metallic materials. I. Macro appearance," Color Res. Appl. **21**, 292–304 (1996).
2. C. S. McCamy, "Observation and measurement of the appearance of metallic materials. II. Micro appearance," Color Res. Appl. **23**, 362–373 (1998).

3. H. Tabata, K. Kumazawa, M. Funakawa, J. Takimoto, and M. Akimoto, "Microstructures and optical properties of scales of butterfly wings," Opt. Rev. **3**, 139–145 (1996).
4. A. R. Parker, "515 million years of structural colour," J. Opt. A Pure Appl. Opt. **2**, R15–R28 (2000).
5. P. Vukusic and J. R. Sambles, "Photonic structures in biology," Nature **424**, 852–855 (2003).
6. F. W. Billmeyer and J. G. Davidson, "Color and appearance of metallized paint films. I. Characterization," J. Paint Technol. **46**, 31–37 (1974).
7. P. A. Lewis, *Pigment Handbook, Properties and Economics*, 2nd ed. (Wiley, 1988), Vol. 1, p. 976.
8. H. G. Völz, *Industrial Color Testing, Fundamentals and Techniques*, 2nd ed. (Wiley, 2001), p. 388.
9. W. R. Cramer, "Examples of interference and the color pigment mixtures green with red and red with green," Color Res. Appl. **27**, 276–281 (2002).
10. G. Baba and H. Arai, "Gonio-spectrophotometry of metal-flake and pearl-mica pigmented paint surfaces," in *Fourth Oxford Conference on Spectroscopy*, A. Springsteen and M. Pointer, eds., Proc SPIE 4826, 79–86 (2003).
11. M. Mikula, M. Ceppan, and K. Vasko, "Gloss and goniocolorimetry of printed materials," Color Res. Appl. **28**, 335–342 (2003).
12. M. E. Nadal and E. A. Early, "Color measurements for pearlescent coatings," Color Res. Appl. **29**, 38–42 (2004).
13. M.V. Diamantini, B. del Curto, and M. Pedeferri , "Interference colors of thin oxide layers on titanium," Color Res. Appl. **33**, 221–228 (2008).
14. G. Wyszecki and W. S. Stiles, *Color Science: Concepts and Methods, Quantitative Data and Formulae*, 2nd ed. (Wiley, 1982), p. 950.
15. DIN 6175-2, "Farbtoleranzen für Automobillackierungen—Teil 2: Effektlackierungen," (Deutsches Institut für Normung e.V., 2001).
16. ASTM E2175-01, "Standard practice for specifying the geometry of multiangle spectrophotometers," (American Society for Testing and Materials, 2001).
17. A. Takagi, A. Watanabe, and G. Baba, "Prediction of spectral reflectance factor distribution of automotive paint finishes," Color Res. Appl. **30**, 275–282 (2005).
18. L. T. Maloney, "Evaluation of linear models of surface spectral reflectance with small numbers of parameters," J. Opt. Soc. Am. A **3**, 1673–1683 (1986).
19. J. Romero, A. Garcia-Beltran, and J. Hernandez-Andres, "Linear bases for representation of natural and artificial illuminants," J. Opt. Soc. Am. A **14**, 1007–1014 (1997).
20. A. Garcia-Beltran, J. L. Nieves, J. Hernandez-Andres, and J. Romero, "Linear bases for spectral reflectance functions of acrylic paints," Color Res. Appl. **23**, 39–45 (1998).
21. L. T. Maloney, "Physics-based approaches to modeling surface color perception," in *Color Vision: From Genes to Perception*, K. R. Gengenfurtner and L. T. Sharpe, eds. (Cambridge University, 1999), pp. 387–422.
22. O. Kohonen, J. Parkkinen, and T. Jaaskelainen, "Databases for spectral color science," Color Res. Appl. **31**, 381–390 (2006).
23. S. M. Nascimento, D. H. Foster, and K. Amano, "Psychophysical estimates of the number of spectral-reflectance basis functions needed to reproduce natural scenes," J. Opt. Soc. Am. A **22**, 1017–1022 (2005).
24. D. Y. Tzeng and R. S. Berns, "A review of principal component analysis and its applications to color technology," Color Res. Appl. **30**, 84–98 (2005).
25. N. Ohta, "Estimating absorption-bands of component dyes by means of principal component analysis," Anal. Chem. **45**, 553–557 (1973).
26. J. A. Worthey and M. H. Brill, "Principal components applied to modeling: dealing with the mean vector," Color Res. Appl. **29**, 261–266 (2004).
27. R. S. Berns, "A generic approach to color modeling," Color Res. Appl. **22**, 318–325 (1997).
28. E. Hecht and A. Zajac, *Optics* (Addison-Wesley, 1974), p. 565.
29. L. P. Sung, M. E. Nadal, M. E. McKnight, E. Marx, and B. Laurenti, "Optical reflectance of metallic coatings: effect of aluminum flake orientation," J. Coat. Technol. **74**, 55–63 (2002).
30. H. J. A. Saris, R. J. B. Gottenbos, and H. Vanhouwelingen, "Correlation between visual and instrumental color differences of metallic paint films," Color Res. Appl. **15**, 200–205 (1990).
31. W. Press, S. Teukolsky, W. Vetterling, and B. Flannery, *Numerical Recipes in C* (Cambridge University, 1992), p. 994.
32. E. Kirchner, G. J. van den Kieboom, L. Njo, R. Super, and R. Gottenbos, "Observation of visual texture of metallic and pearlescent materials," Color Res. Appl. **32**, 256–266 (2007).
33. B. Gralak, G. Tayeb, and S. Enoch, "Morpho butterflies wings color modeled with lamellar grating theory," Opt. Express **9**, 567–578 (2001).
34. S. Yoshioka and S. Kinoshita, "Polarization-sensitive color mixing in the wing of the Madagascan sunset moth," Opt. Express **15**, 2691–2701 (2007).
35. F. W. Billmeyer and E. C. Carter, "Color and appearance of metallized paint films. II. Initial application of turbid-medium theory," J. Coat. Technol. **48**, 53–60 (1976).